Water Environment Federation
the water quality people

The influence of wind in secondary settling tanks for wastewater treatment – A computational fluid dynamics study. Part II: Rectangular secondary settling tanks

Haiwen Gao , Michael K. Stenstrom*

Department of Civil and Environmental Engineering, University of California Los Angeles, Los Angeles, California

Received 11 April 2019; Revised 17 September 2019; Accepted 19 September 2019

Correspondence to: Michael K. Stenstrom, Department of Civil and Environmental Engineering, University of California Los Angeles, Los Angeles, CA.
Email: stenstro@seas.ucla.edu

*WEF Member/Fellow.

Published online 06 October 2019 in Wiley Online Library (wileyonlinelibrary.com)

DOI: 10.1002/wer.1244

• **Abstract**

Computational fluid dynamics (CFD) model is used to study the effect of wind on the performance of a rectangular secondary sedimentation tank (SST) in a wastewater treatment plant (WWTP). Unlike most of the previous CFD modeling studies which evaluated the wind effect on the sedimentation tank in only water treatment plants, this study evaluates a rectangular SST in a WWTP at different wind speeds and directions, and under different inflow loading conditions. The wind is qualitatively and quantitatively analyzed for a range of wind speeds and directions as well as loading rates. The net effect is to change the three-dimensional hydrodynamics profiles, effluent suspended solids, and sludge blanket height. The simulation results show that the wind deteriorates overall clarification performance of the rectangular SST and has little effect on the sludge thickening under mild wind conditions until the speed increases an extreme windy condition. These CFD simulation results suggest that in strong windy climates, covering SSTs or protecting them from strong winds may be justified. © 2019 Water Environment Federation

• **Practitioner points**

- This is the first comparison of wind effects on a rectangular secondary sedimentation tank
- The effects of varied flow conditions, wind directions, and velocities are compared
- Wind-induced currents in the settling tank negatively affect removal efficiency
- Winds have strong negative impact on the performance of sedimentation tanks

• **Key words**

computational fluid dynamics; secondary settling tank; turbulent flow; wastewater treatment plant

Introduction

In conventional wastewater treatment facilities, aeration tanks are used with secondary settling tanks (SSTs) to remove organic matter and reduce nutrients such as nitrogen and phosphorous. Secondary settling tanks (SSTs), also known as secondary sedimentation tanks or secondary clarifiers, have two different functions: clarification and thickening (Parker, 1983). Clarification separates the suspended solids from the effluent while thickening concentrates the solids at the tank bottom in order to recycle or dispose with less volume (Gao & Stenstrom, 2017).

In the last three decades, many researchers and engineers have studied influential factors on the efficiency of SSTs and optimized the performance of SSTs with computational fluid dynamics (CFD) models. Zhou and McCorquodale (1992a) were among the first to use CFD to study SSTs and evaluated underflow hydrodynamics of a circular SST using their 2D CFD model. After overcoming the strong local numerical instabilities near the inlet baffle, they were able to model the entire SST, from inlet zone to effluent weir. After Zhou and McCorquodale (1992a), there have been a growing number of CFD evaluations of SSTs in wastewater treatment plants, and some of the major ones are summarized in Table 1.

The effects of wind on the rectangular SST are investigated in this study and differ from most of the previous CFD studies on SSTs, which focused on influential factors inside the SST, such as internal geometry, sludge settling properties, flow conditions, McCorquodale, Motta, Griborio, Georgiou, and Homes (2004) showed that the efficiency of the SSTs depends on several influential factors, including atmospheric condition, such as wind velocity. However, they did not study the wind shear effects on the performance of SSTs with their Q3D model and they concluded that SST models should be expanded to three-dimensional (3D) to accurately predict wind effects.

The effects of wind on settling tanks for water treatment plants (WTPs) have been analyzed in several recent studies (Gkesouli, Nitsa, Stamou, Rutschmann, & Bui, 2016; Gkesouli & Stamou, 2018; Goodarzi, Lari, & Alighardashi, 2018; Khezri, Biati, & Erfani, 2012; Stamou & Gkesouli, 2015). Gao and Stenstrom (2019c) summarized the major conclusions of these studies. In most cases, the predicted effects on removal efficiency are negative. However, since the effects of particle concentration on the hydrodynamics of settling tanks in WTPs are negligible, whereas the high particle concentration in the influent of SSTs in WWTPs makes the flow currents density-driven, the hydrodynamics for settling tanks in WTPs and SSTs in WWTPs are different. Therefore, the results for WTP settling tanks cannot be extrapolated to SSTs in WWTPs.

In this part of the study, the wind effects on the performance of a rectangular SST in the WWTP are investigated over the range of different wind velocities, directions, and flow conditions. This work is a sequel of a previous work (Gao & Stenstrom, 2019c) in which we studied the wind effects on the performance of a circular SST in the WWTP.

In recent years, several researchers have analyzed the wind effects on settling tanks for water treatment plants (WTPs) (Gkesouli et al., 2016; Gkesouli & Stamou, 2018; Goodarzi et al., 2018; Khezri et al., 2012; Stamou & Gkesouli, 2015). Table 1 shows the major conclusions of these studies. In most cases, the predicted effects on removal efficiency are negative, with the exception of low counter-current wind velocity, which increased ESS removal efficiency. However, the applicability of these studies to SSTs in WWTPs is limited since the particle concentration in the influent of the settling tank in WTPs is very low. The effects of particles at low concentration on the flow field are negligible, whereas the high particle concentration in the influent of SSTs in WWTPs makes the flow currents density-driven. Therefore, the flow and concentration fields for settling tanks in WTPs and SSTs in WWTPs are different, and results concluded for settling tanks in WTPs may not be appropriate for SSTs in WWTPs. To the best of our knowledge, none of the published papers simulated the wind effects on SSTs in WWTPs.

This study differs from the previous wind studies on settling tanks in WTPs in that, first of all, the rectangular SST is studied under different flow rates and wind directions and wind velocities. Additionally, high total suspended solids concentrations (TSS) concentration-induced density currents are considered. Wicklein and Samstag (2009) compared the accuracy of the standardized multiphase model based on a theoretical solution for slip velocity based on particle size and the particle transport model based on sludge settling velocities to predict the SST hydrodynamics profiles. The former model is often used to simulate the hydrodynamics characteristics of settling tanks in WTPs (Gkesouli et al., 2016; Goodarzi et al., 2018; Stamou & Gkesouli, 2015), whereas the second model is often used in SST predictions. Their study showed that since the flow in SST is driven by density currents, the particle transport model based on sludge settling velocities perform better than the standardized multiphase model. Therefore, the particle transport model based on sludge settling velocities used in our previous SST studies (Gao & Stenstrom, 2018a, 2018b, 2019c) is also coupled in this current study.

The geometry of SST and flow conditions is adapted from Krebs, Stamou, Garcia-Heras, and Rodi (1996). The CFD package ANSYS Fluent v18.2 is used to simulate the wind effects co-current, counter-current, and perpendicular to the SST longitudinal direction, and Tecplot 360 is used for 3D hydrodynamics analysis. Under each tested wind direction, the current velocity on the water surface (U_s) increases from zero to two mildly windy conditions (U_s = 0.125 and 0.25 m/s), and one extreme condition (U_s = 0.50 m/s), which correspond to 8.35, 16.69, and 33.39 miles/hr for the wind velocities at 10 m height (U_{10}) or "tree top" wind velocities, respectively. Equation (1) shows the conversion between U_s and U_{10} (Gkesouli & Stamou, 2018).

$$U_s = (0.9\% - 5.8\%)\, U_{10} \tag{1}$$

The impact of wind is qualitatively and quantitatively compared to three-dimensional hydrodynamics profiles and ESS and sludge blanket height (SBH) in the range of different wind speeds, directions, and flow conditions.

Methodology

Governing equations

Since this work is a sequel of our previous work, only the turbulence model is shown below. A more detailed description of 3D transient CFD model non-Newtonian turbulent flow behavior in an SST can be found in the previous work.

The equations describing 3-D, transient, turbulent, and density stratified flow in an SST are as follows (Das et al., 2016):

Continuity equation:

$$\frac{\partial \rho}{\partial t} + \nabla \cdot \left(\rho \overrightarrow{u_l}\right) = 0 \tag{2}$$

Momentum equation:

$$\frac{\partial \rho \overrightarrow{u_l}}{\partial t} + \nabla \cdot \left(\rho \overrightarrow{u_l} \overrightarrow{u_l}\right) = -\nabla p + \nabla \cdot \overline{\overline{\tau}} + \vec{F} \tag{3}$$

Table 1. Summary of previous CFD SST studies

REFERENCES	DIM.	MODEL	VALIDATION	REMARKS
Zhou and McCorquodale (1992a)	2D	URANS+*sk*-ε	Velocity profiles	First model of the entire SST, from inlet zone to effluent weir
Zhou and McCorquodale (1992b)	2D	URANS+*sk*-ε	Velocity profiles	Evaluated the effects of inlet baffle locations on the SST removal efficiency
Vitasovic, Zhou, McCorquodale, and Lingren (1997)	2D	URANS+*sk*-ε	Performance indicators	Evaluated the effects of surface overflow rate and surface loading rate on SST performance
De Clercq (2003)	2D	URANS+*sk*-ε	Velocity/concentration profiles	Developed an advanced sludge rheological submodel for the SST CFD model
Weiss, Plósz, Essemiani, and Meinhold (2007)	2D	URANS+*sk*-ε	Concentration profiles	Analyzed the sludge rheological behavior in the SST
Ramalingam et al. (2012)	3D	URANS+*sk*-ε	Tracer test	Developed a new method to measure discrete floc settling velocities and used it in their modified flocculation model
Das et al. (2016)	3D	URANS+*sk*-ε	None	Showed how inlet geometry modifications can reduce ESS by more than 80%
Gao and Stenstrom (2018a)	2D	RANS+*sk*-ε	Velocity/concentration profiles	Showed the effect of three different turbulence models on the prediction of velocities near the SST inlet zone and near the sludge hopper

where ρ is the local fluid density, t is time, $\vec{u_i}$ is the absolute velocity vector, p is the general pressure less the hydrostatic pressure at reference density ρ_r, $\overline{\overline{\tau}}$ is viscous stress, and $\vec{F}$ is body force.

Local fluid density:

$$\rho = \rho_r + C\left(1 - \frac{\rho_r}{\rho_p}\right) \quad (4)$$

Standard k-ε turbulence model:

$$\frac{\partial \rho k}{\partial t} + \rho\nabla\left(\vec{u_i}k\right) = \rho\nabla\left[\left(\nu + \frac{\nu_t}{\sigma_k}\right)\nabla k\right] + G_k + G_b - \rho\varepsilon \quad (5)$$

$$\frac{\partial \rho\varepsilon}{\partial t} + \rho\nabla\left(\vec{u_i}\varepsilon\right) = \rho\nabla\left[\left(\nu + \frac{\nu_t}{\sigma_\varepsilon}\right)\nabla\varepsilon\right] + C_1\frac{\varepsilon}{k}\left(G_k - C_3G_b\right) - C_2\rho\frac{\varepsilon^2}{k} \quad (6)$$

in which k and ε are turbulent kinetic energy (TKE) and turbulent dissipation rate, respectively. G_k represents the generation of TKE due to the mean velocity gradients, and G_b corresponds to the generation of TKE due to buoyancy. ϑ is the viscosity of the sludge mixture; ϑ_t is the turbulent eddy viscosity.

The turbulent viscosity, ϑ_t, is determined as a function of TKE and TDR by,

$$\vartheta_t = C_\mu\frac{k^2}{\varepsilon} \quad (7)$$

Sludge transport equation:

$$\frac{\partial \rho C}{\partial t} + \frac{\partial \rho\left(\vec{u_i} + V_s\right)C}{\partial x_i} = \rho\frac{\partial}{\partial x_i}\left(\frac{\nu_t}{\sigma_c}\frac{\partial C}{\partial x_i}\right) \quad (8)$$

where C is the sludge concentration and V_s is the sludge settling velocity in the vertical direction.

Sludge rheological model (Bokil, 1972):

$$\nu = 1\times10^{-6}e^{1.386C} \text{ for } C \le 1 \text{ g/L} \quad (9)$$

and

$$\nu = 2.9\times10^{-6}e^{0.322C} \text{ for } C \ge 1 \text{ g/L}$$

Sludge settling equation (Takács, Patry, & Nolasco, 1991):

$$V_s = \max\left(0, V_o\left(e^{-r_p(C - C_{min})} - e^{-r_h(C - C_{min})}\right)\right) \quad (10)$$

r_p and r_h account for rapidly and poorly settling floc, respectively. They were calibrated in the original study of this rectangular SST (Krebs et al., 1996). The predictions of the horizontal velocity profiles were also calibrated with the laboratory experiments in the original study.

CFD boundary conditions

Boundary conditions are shown in Table 2. Compared with our previous studies (Gao & Stenstrom, 2018a, 2018b, 2019a, 2019b), the only different boundary condition needed to simulate the windy conditions is the surface boundary condition, which is a constant horizontal velocity as the free surface along the wind direction (Gkesouli et al., 2016; Stamou & Gkesouli, 2015).

Numerical simulations

The governing equations are solved using the commercial CFD package ANSYS Fluent 18.2. The fluid flow equations are solved using the SIMPLE algorithm. Second-order upwind methods are used for spatial discretization, whereas first-order implicit methods are used for temporal discretization. For the CFD simulations, a 10^{-3} reduction in residuals is set as the tolerance criterion for the iterations in each time step. The concentration of solids at the effluent, sludge hopper, and the total solids volume are used as the convergence indicators. The typical time for convergence to an acceptable level of accuracy is around 2 days on a workstation with 16 Xeon Sliver 4114 processors.

In numerical simulations, when the water surface is considered as a “rigid-lid,” the initial position of the water surface should be given accurately; otherwise, it will cause errors in calculation. The initial position of water surface can be determined by experiment (Jonhn & Joseph, 2002) and by the theory of multiphase flow with VOF method (Liu, Wei, Lv, & Yang, 2014; Wei, Liu, & Lv, 2016). Here, consistent to the numerical solution procedures shown in Stamou and Gkesouli (2015), and Gkesouli and Stamou (2018), the converged solution under no wind condition is used as the initial condition under the windy condition. Since this is the first study of wind effects on SSTs in WWTPs, in the future study, more advanced method, such as the volume of fluid (VOF) method (Liu et al., 2014; Wei et al., 2016), will be used to more accurately describe the surface effects.

The sludge settling equation is calibrated in the original study of this rectangular SST (Krebs et al., 1996). The predictions of the horizontal velocity profiles are also calibrated with the laboratory experiments in the original study.

Figure 1 shows the geometries, dimensions, the tested flow conditions, and meshes for the rectangular SST. The computational mesh is generated from Trelis 16.5 (American Fork, UT) and consists of a total number of 2 million hybrid cells. The geometry of the rectangular SST was cut longitudinally and automatically shown with different colors. The sections with different colors along the longitudinal direction represent the mesh in different sizes, with finer meshes in the field near the inlet and outlets and coarser meshes in the main settling zone.

In order to ensure that the solutions are mesh-independent, one coarser mesh consisting of 1 million cells, and a finer one consisting of 4 million cells are used for the SST. Figure 2 shows velocity magnitudes as a function of depth for the SST calculated from meshes with different grid numbers at three longitudinal locations (near the inlet, at the main settling zone, near the outlet). Since the differences in results using the medium and fine meshes are negligible, solution from the mesh of 2 million cells for the SST is considered mesh-independent and has the benefit of increased computational speed.

Table 2. Numerical boundary conditions used in this study

BOUNDARY TYPES	CALM CONDITION	WINDY CONDITION
Inlet	Velocity inlet	Velocity inlet
Sludge bottom	Velocity inlet	Velocity inlet
Effluent	Pressure outlet	Pressure outlet
Surface	Free slip wall	Moving wall with a no slip-shear condition
Wall	Stationary walls with a no slip-shear condition	Stationary walls with a no slip-shear condition

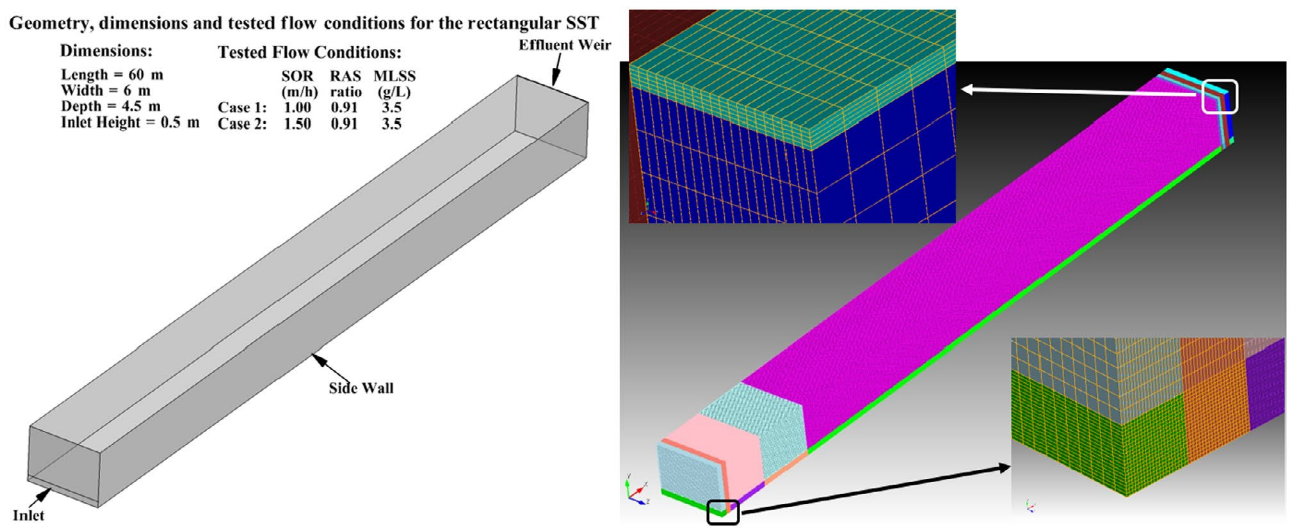

Figure 1. Geometry, dimensions, the tested flow conditions (left) and mesh (right) for the rectangular SST.

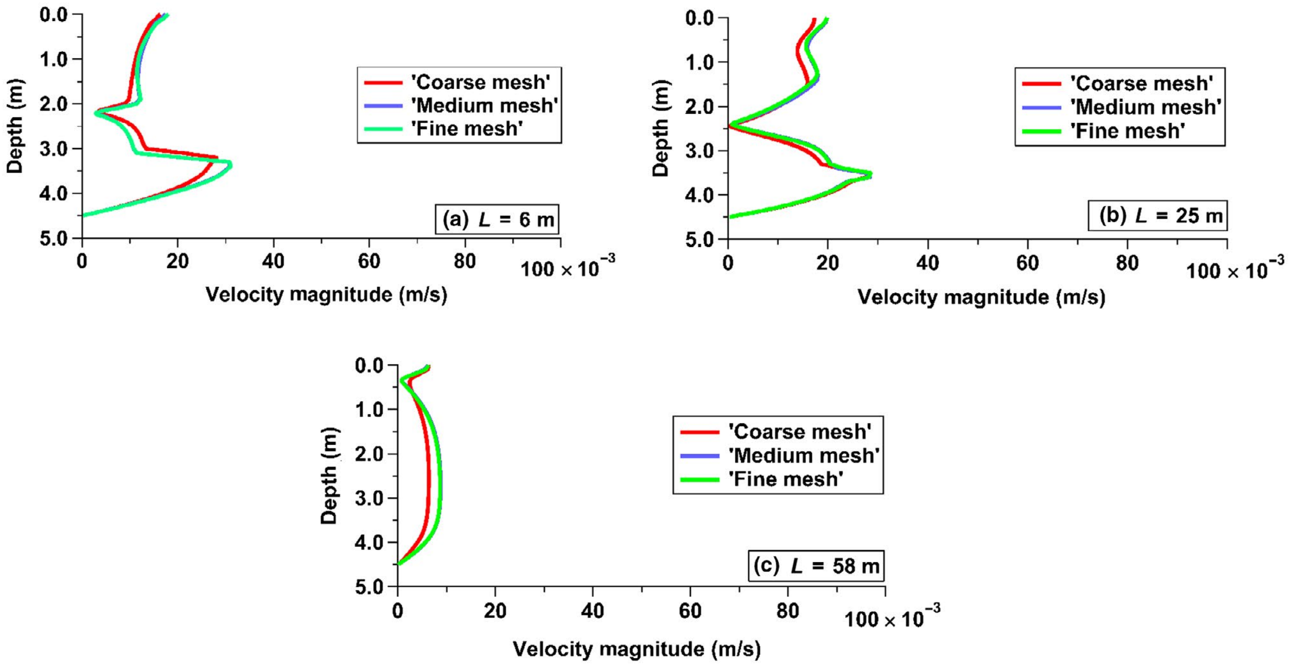

Figure 2. Grid independence test for calculated velocity magnitude (m/s) at three representative longitudinal locations of the rectangular SST.

Results and Discussion

Impact of the wind on the rectangular SST

Performance indicators. Figure 3 compares the predicted area-weighted ESS and SBH among different current velocity on the water surface for Cases 1 and 2. It shows that among these three different types of wind directions (co-current, counter-current, perpendicular to SST longitudinal direction), counter-current wind has the most significant negative impact on the SST clarification, while co-current wind slightly reduces the ESS under the first mild windy condition, but performance gradually deteriorates with increasing wind speed. The wind flowing perpendicular to the SST's longitudinal direction has the least negative effect on the SST clarification. However, neither these three types of wind have strong impact on the sludge thickening under the mild windy conditions (U_s = 0.125 and 0.25 m/s), and only co-current and counter-current wind has strong impact on the sludge thickening under the extreme windy condition.

Table 3 shows the range of ESS predictions in the clam and different windy conditions for Cases 1 and 2. It also shows that under the first mild windy condition (U_s = 0.125 m/s), co-current wind slightly improves clarification of the SST along the entire length of the effluent weir, whereas the counter-current wind increases ESS to more than 30 mg/L at certain location along the effluent weir. Also, when wind increases perpendicularly to SST longitudinal direction, the highest ESS increases gradually to 30 mg/L at the extreme windy condition.

Variation of the hydrodynamics as the existence of co-current wind. Figure 4 compares the velocity profiles under the calm and co-current wind conditions for Case 2. Under the calm condition (Figure 4a), the inflow generates a strong horizontal jet from the inlet to the rear of the tank, which creates a current flowing counterclockwise over the length of the entire SST and forms a small eddy recirculating clockwise near the effluent weir. However, the existence of co-current wind (Figure 4b) changes the flow pattern above the horizontal inflow jet. It changes the recirculation over the entire SST to flow clockwise and enhances the size and turbulence intensity of the eddy near the effluent weir. Since the recirculation direction above the horizontal inflow jet is opposite to the eddy near the effluent weir, it suppresses the upward flow of the suspended solids to the effluent weir. As the current velocity on the water surface increases (Figure 4c,d), recirculation over the entire SST and near the effluent weir is intensified. When flow velocities on the water surface increase to 0.5 m/s (extreme condition), the current velocity on the entire water depth near the rear wall increases to the same magnitude of the inlet velocity. The strong current velocity near the rear wall stirs up the suspended solids to the effluent weir and causes the SST to fail.

Figure 5 shows the comparison of concentration iso-surfaces at 30 mg/L under the calm and co-current wind conditions. Similar to the velocity patterns shown in Figure 4, Figure 5a shows that under the calm condition, the elevation of the concentration iso-surface reduces gradually as the sedimentation of suspended solids along the longitudinal direction. However, the existence of surface current velocity caused by the co-current wind (Figure 5b) intensifies the eddy near the effluent weir, therefore stirring up the suspended solids near the effluent weir to a higher elevation. As the increase of surface current velocity (Figure 5c,d), the intensification of the

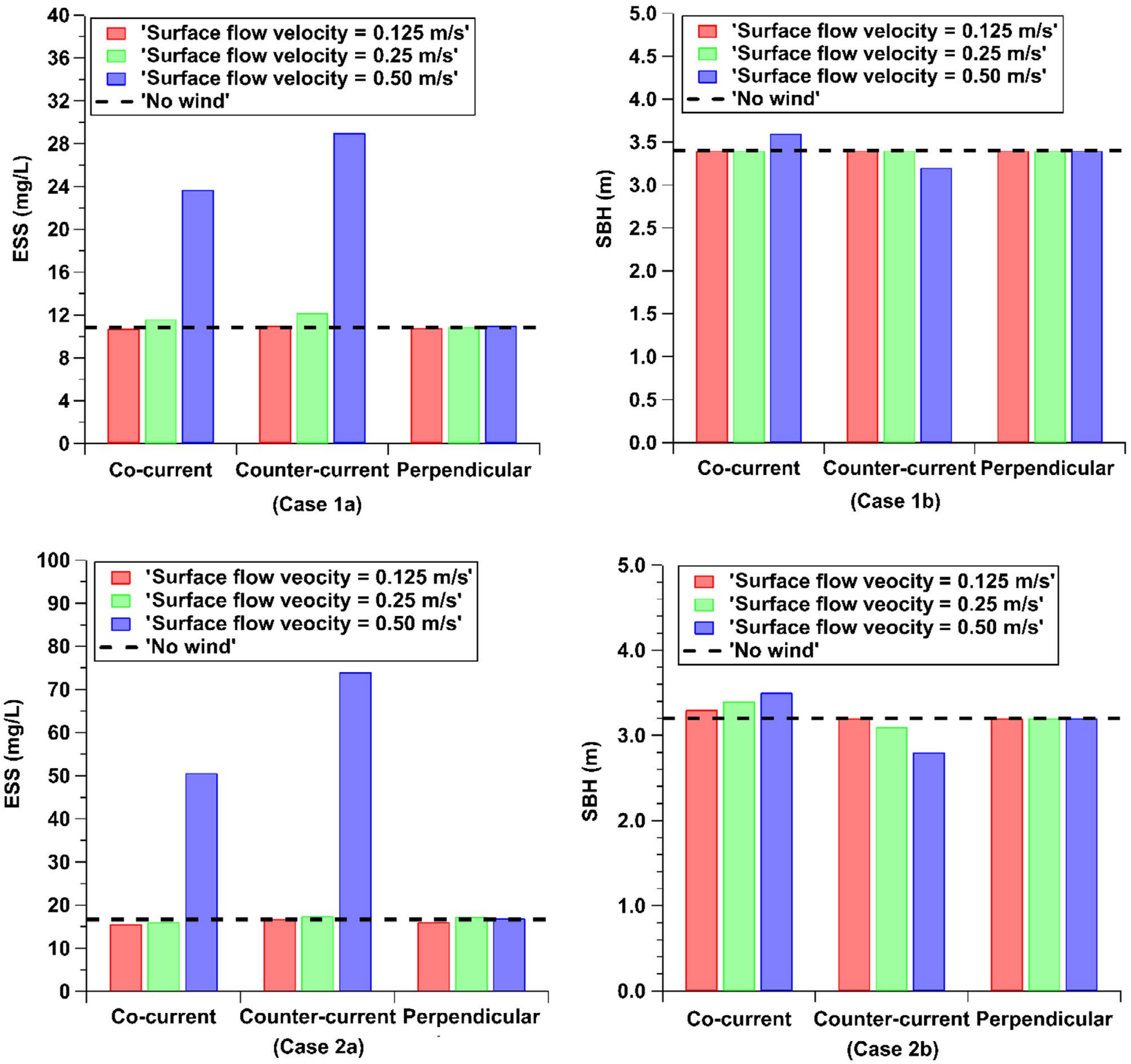

Figure 3. Predictions of area-weighted ESS and SBH among different flow velocities on water surface for Cases 1 and 2.

recirculation above the horizontal jet and the eddy near the effluent weir stir up the suspended solids over the entire SST; therefore, the entire elevation of the iso-surface is increased. Figure 5d shows that the eddy near the effluent weir is so strong that the ESS concentration along the entire length of the effluent weir is more than 30mg/L (ESS limiting).

Variation of the hydrodynamics as the existence of counter-current wind. Figure 6 compares the velocity profiles under the calm and counter-current wind conditions for Case 2. It shows that the existence of surface current velocity caused by the counter-current wind enhances the horizontal inflow jet flowing to the rear wall and then flowing upward to the effluent weir. The stronger upward flow carries the suspended solids to the effluent weir; therefore, counter-current wind has stronger negative impacts than the co-current wind. Also, different from the flow pattern under co-current wind, counter-current wind strengthens the counterclockwise flow pattern over the entire SST, especially near the front wall. As the counter-current wind increases to the extreme condition (Figure 6d), the current velocity on the entire water depth near the front wall increases to the same magnitude of the inlet velocity.

Figure 7 shows the comparison of concentration iso-surfaces at 30 mg/L under the calm and counter-current wind conditions. Similar to the velocity patterns shown in Figure 6, the stronger upward flow near the rear wall (Figure 7b) carries suspended solids to the effluent weir; therefore, the elevation of the concentration iso-surface near the rear wall increases. As the increase of surface current velocity was caused by the counter-current wind (Figure 7c,d), suspended solids on the entire SST

Table 3. Predictions of ESS range among different surface flow velocities for Cases 1 and 2

SURFACE FLOW VELOCITIES	WIND DIRECTIONS	AVERAGED ESS (MG/L)	LOWEST ESS (MG/L)	HIGHEST ESS (MG/L)
Case 1				
$U_s = 0$		10.8	10.3	11.4
$U_s = 0.125$ m/s	Co-current	10.7	10.2	10.8
$U_s = 0.25$ m/s	Co-current	11.6	10.5	12.0
$U_s = 0.50$ m/s	Co-current	23.7	14.0	31.0
$U_s = 0.125$ m/s	Counter-current	11.0	11.0	11.6
$U_s = 0.25$ m/s	Counter-current	12.2	12.0	13.0
$U_s = 0.50$ m/s	Counter-current	29.0	18.9	56.6
$U_s = 0.125$ m/s	Perpendicular	10.8	10.0	11.0
$U_s = 0.25$ m/s	Perpendicular	10.9	10.0	11.4
$U_s = 0.50$ m/s	Perpendicular	11.0	10.3	11.4
Case 2				
$U_s = 0$		16.6	14.3	21.0
$U_s = 0.125$ m/s	Co-current	15.6	10.0	23.0
$U_s = 0.25$ m/s	Co-current	16.0	11.0	20.0
$U_s = 0.50$ m/s	Co-current	50.6	19.6	69.4
$U_s = 0.125$ m/s	Counter-current	16.8	15.0	32.0
$U_s = 0.25$ m/s	Counter-current	17.4	15.8	22.5
$U_s = 0.50$ m/s	Counter-current	74.0	49.0	136
$U_s = 0.125$ m/s	Perpendicular	16.0	13.0	19.0
$U_s = 0.25$ m/s	Perpendicular	17.3	12.4	25.0
$U_s = 0.50$ m/s	Perpendicular	16.9	12.5	27.7

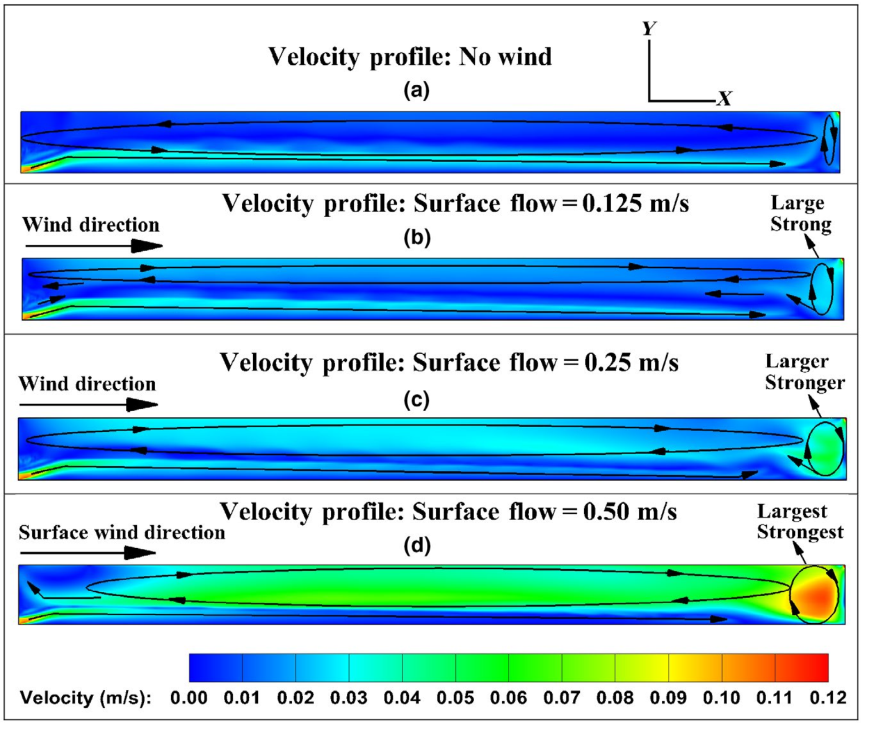

Figure 4. Comparison of velocity profiles under the calm and co-current wind conditions for Case 2.

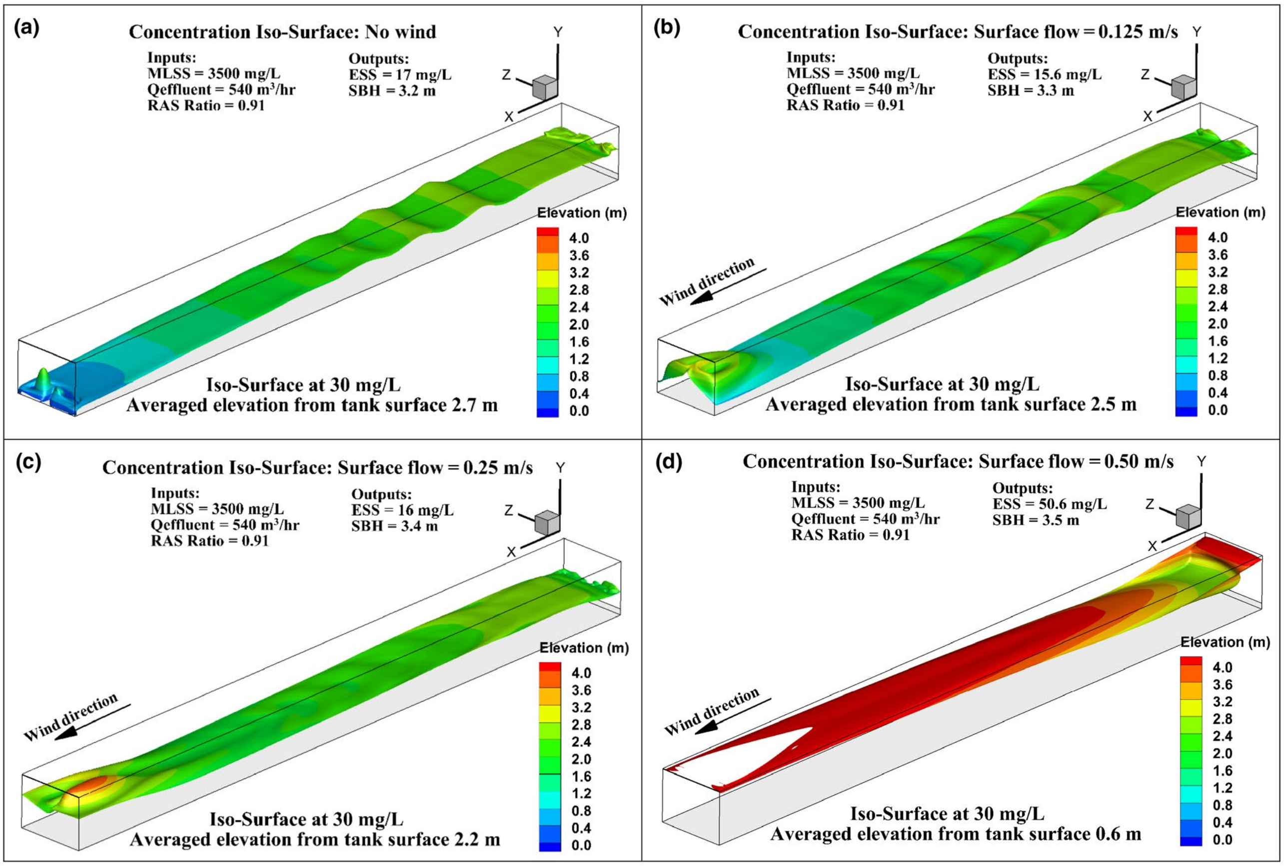

Figure 5. Comparison of concentration iso-surfaces at 30 mg/L under the calm and co-current wind conditions for Case 2.

are stirred up and the entire elevation of the concentration iso-surface is increased. Figure 7d shows that the concentration of the suspended solids is more than 30 mg/L (ESS limiting) on a significantly larger scale of SST surface area than under the same velocity of co-current wind (Figure 5d), which also indicates that the counter-current wind has stronger negative impacts than the co-current wind on the SST.

Compared with the wind study of Gkesouli et al. (2016) for a settling tank in the WTP which shows that co-current wind has negligible negative effects and counter-current wind has positive effects on the particle removal efficiency, the current study shows that the SST fails with only 0.125 m/s increase of surface current velocity caused by the counter-current wind velocity and 0.25 m/s increase of surface current velocity caused by the co-current wind velocity.

Variation of the hydrodynamics as the existence of wind flows perpendicular to the SST longitude direction. Figure 8 shows the comparison of concentration iso-surfaces at 30 mg/L under the calm condition and wind flows perpendicular to the tank longitudinal direction for Case 2. It shows that the concentration of the iso-surfaces at 30 mg/L under the first windy condition ($U_s = 0.125$ m/s) and under the calm condition is similar, which indicates that the suspended solid distribution in the rectangular SST is insensitive to the wind velocity less or equal than this mild windy condition. As the current velocity on the water surface increase to 0.25 m/s, the suspended solids on the downwind side of the effluent weir is stirred up and elevated close to the effluent weir. When the surface current velocity increases to 0.50 m/s (extreme condition), the concentration iso-surface is elevated close to the effluent weir on the entire width of the SST.

Conclusions

In this study, Fluent-based 3D numerical models are used to analyze the impact of wind on the performance of a rectangular SST in the WWTP. The rectangular SST is tested under two different flow conditions (Cases 1 and 2). Under each flow condition, three different wind speeds as well as three different wind directions (co-current, counter-current wind, and wind flowing perpendicular to the SST long axis) are tested. Therefore, 18 simulations are run for the rectangular SST.

The predictions of performance indicators, such as ESS and SBH, 2D velocity profiles, and 3D concentration iso-surface 3D hydrodynamics profiles, are compared under different wind velocities and flow conditions. Additionally, predictions under different wind directions are also compared.

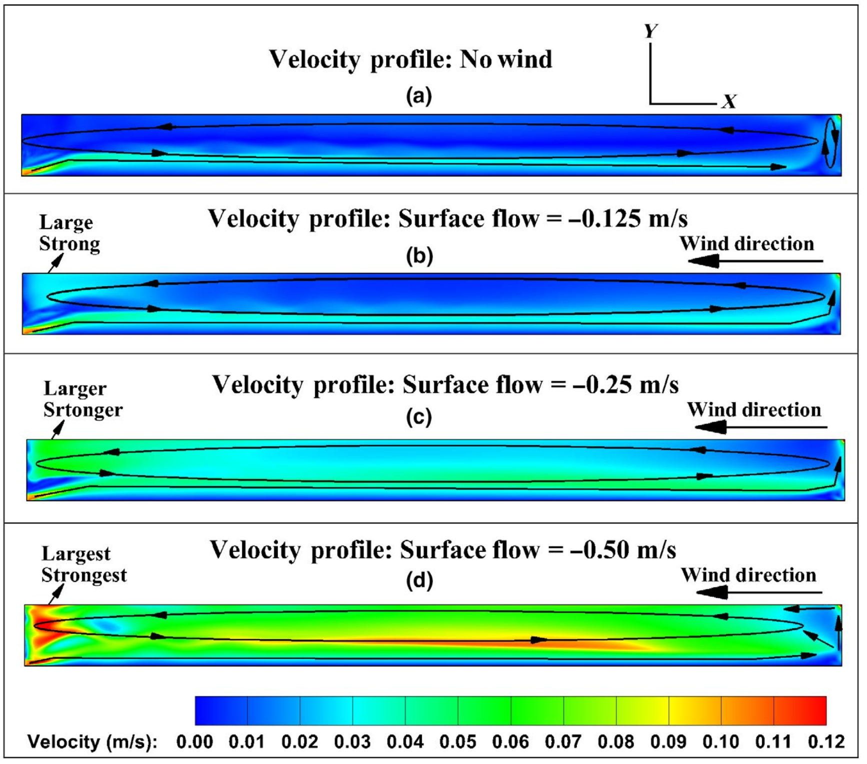

Figure 6. Comparison of velocity profiles under the calm and counter-current surface wind conditions for Case 2.

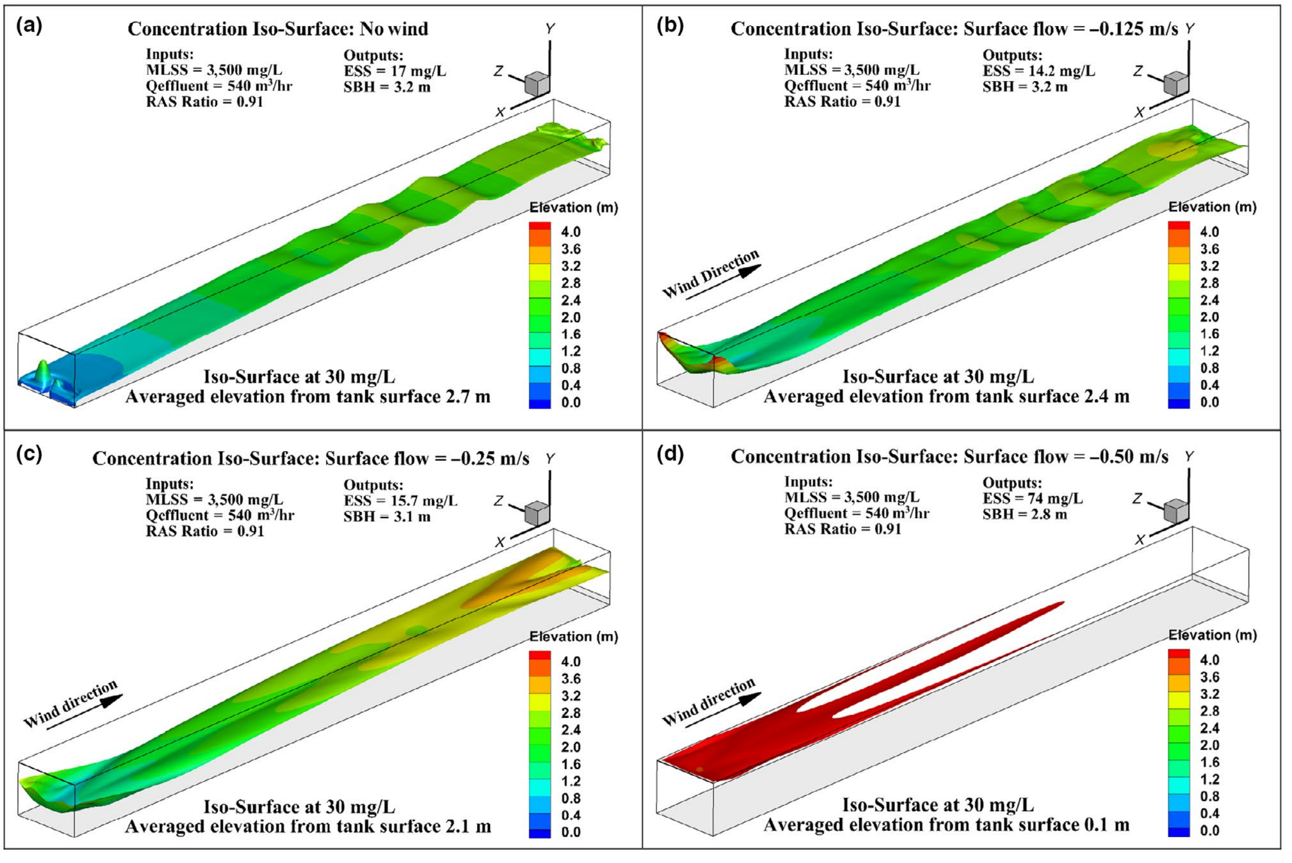

Figure 7. Comparison of concentration iso-surfaces at 30 mg/L under the calm and counter-current surface wind conditions for Case 2.

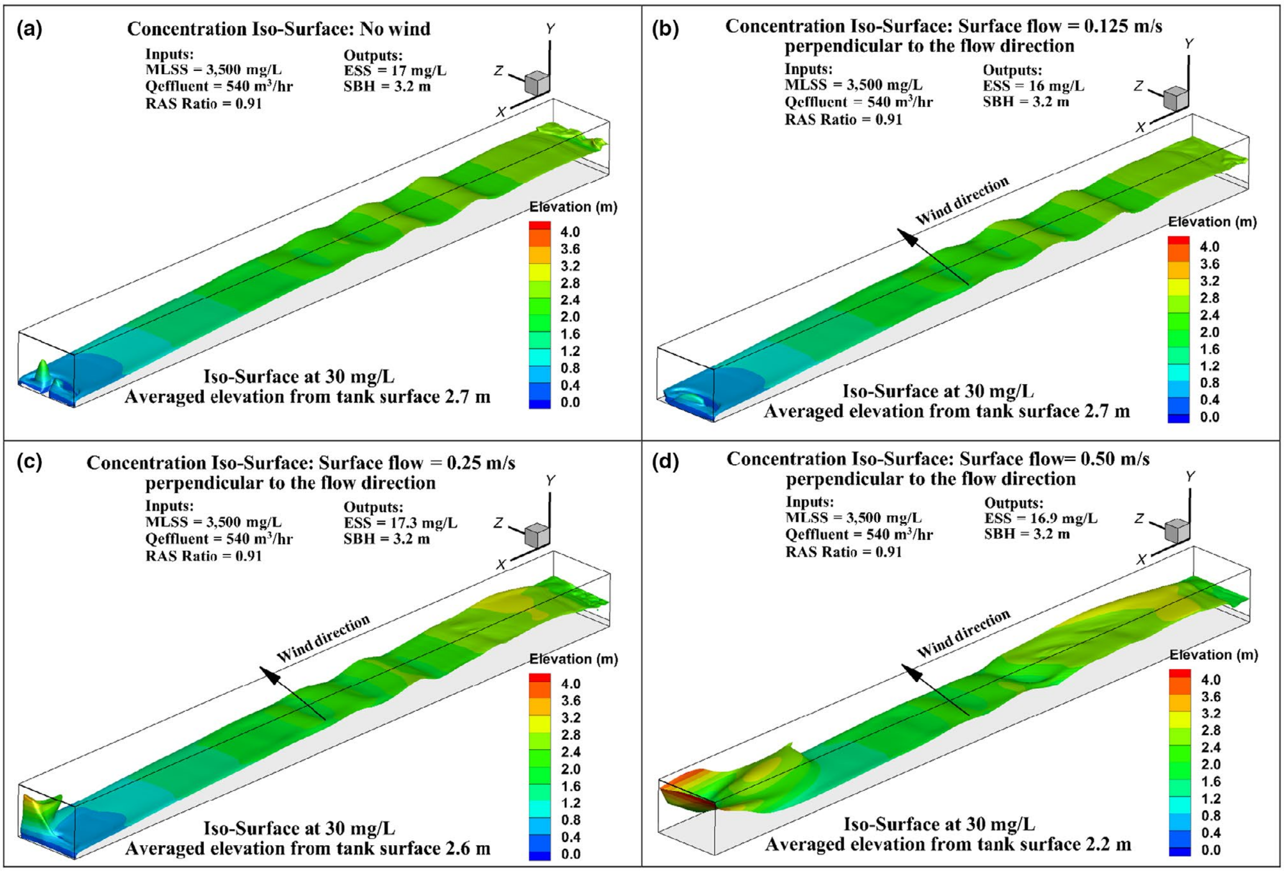

Figure 8. Comparison of concentration iso-surfaces at 30 mg/L under the calm condition and surface wind flows perpendicular to the tank longitudinal direction for Case 2.

For the cases studied under various flow conditions, wind speeds, and wind directions, the following predictions and conclusions are made:

- Wind deteriorates the SST clarification performance under every wind direction in the rectangular SST, except with mild co-current windy condition ($U_s \leq 0.125$m/s), which slightly improves the clarification of the rectangular SST.
- Counter-current wind has strongest negative impacts on the SST while the wind flowing perpendicular to the SST longitudinal direction has the least negative impacts.
- Wind under the mild windy conditions ($U_s \leq 0.25$m/s) has little effect on the sludge thickening under every wind direction, while it deteriorates the sludge thickening under the extreme windy condition ($U_s = 0.50$m/s).
- These results suggest that in strong windy climates covering rectangular SSTs or protecting them from strong winds may be justified.

Data availability statement

The three programs we used are commercially available and we have referenced them. The calibration data are from a previously published study (Krebs et al., 1996), which we have referenced, and are available on Web of Science and Google Scholar databases.

References

Bokil, S. D. (1972). *Effect of mechanical blending on the aerobic digestion of the waste activated sludge*. Ph.D. thesis, Department of Civil and Engineering. Ontario, Canada: University of Windsor.

Das, S., Bai, H., Wu, C., Kao, J.-H., Barney, B., Kidd, M., & Kuettel, M. (2016). Improving the performance of industrial clarifiers using three-dimensional computational fluid dynamics. *Engineering Applications of Computational Fluid Mechanics*, *10*(1), 130–144.

De Clercq, B. (2003). *Computational fluid dynamics of settling tanks: Development of experiments and rheological, settling, and scraper submodels*. BIOMATH. Ghent, Belgium: University of Ghent.

Gao, H., & Stenstrom, M. K. (2017). *Computational fluid dynamics applied to secondary clarifier analysis*. In Proceeding of the 17th Annual World Environmental and Water Resources Congress, pp. 301–315. Sacramento, CA. https://doi.org/10.1061/9780784480632

Gao, H., & Stenstrom, M. K. (2018a). Evaluation of three turbulence models in predicting of the hydrodynamics of a secondary sedimentation tank. *Water Research*, *143*, 445–456.

Gao, H., & Stenstrom, M. K. (2018b). Turbulence and interphase mass diffusion assumptions on the performance of secondary settling tanks. *Water Environment Research*, *91*(2), 101–110.

Gao, H., & Stenstrom, M. K. (2019a). Generalizing the effects of the baffling structures on the buoyancy-induced turbulence in secondary settling tanks with eleven different geometries using CFD models. *Chemical Engineering Research and Design*, *143*, 215–225.

Gao, H., & Stenstrom, M. K. (2019b). Evaluating the effects of inlet geometry on the flux capacity of secondary settling tanks with computational fluid dynamics model and one-dimensional flux theory model. *Journal of Environmental Engineering*, *145*(10), 04019065. https://doi.org/10.1061/(ASCE)EE.1943-7870.0001582

Gao, H., & Stenstrom, M. K. (2019c). The influence of wind in secondary settling tanks for wastewater treatment – A computational fluid dynamics study. Part I: circular secondary settling tanks. *Water Environment Research*. (Accepted).

Gkesouli, A., Nitsa, M., Stamou, A., Rutschmann, P., & Bui, M. D. (2016). Modeling the effect of wind in rectangular settling tanks for water supply. *Desalination and Water Treatment*, *57*(54), 26345–26354.

Gkesouli, A., & Stamou, A. (2018). A CFD modeling procedure to assess the effect of wind in settling tanks. *Journal of Hydroinformatics*, *21*(1), 123–135.

Goodarzi, D., Lari, K. S., & Alighardashi, A. (2018). A large eddy simulation study to assess low-speed wind and baffle orientation effects in a water treatment sedimentation basin. *Water Science and Technology*, *2017*(2), 412–421.

Jonhn, F. E., & Joseph, B. F. (2002). *Fluid mechanics with engineering applications*, 10th ed. New York, NY: McGraw-Hill companies, Inc.

Khezri, S. M., Biati, A., & Erfani, Z. (2012). Determination of the effect of wind velocity and direction changes on turbidity removal in rectangular sedimentation tanks. *Water Science and Technology*, *66*(12), 2814–2820.

Krebs, P., Stamou, A., Garcia-Heras, J. L., & Rodi, W. (1996). Influence of inlet and outlet configuration on the flow in secondary clarifiers. *Water Science and Technology*, *34*(5–6), 1–9.

Liu, Y. L., Wei, W. L., Lv, B., & Yang, X. F. (2014). Research on optimal radius ratio of impellers in an oxidation ditch by using numerical simulation. *Desalination and Water Treatment*, *52*(13–15), 2811–2816.

McCorquodale, J. A., La Motta, E., Griborio, A., Georgiou, I., & Homes, J. (2004). *Development of software for modeling activated sludge clarifier system*. Technology Transfer Report Submitted to US EPA, Schielder Urban Environmental System Center, University of New Orleans, New Orleans, LA.

Parker, D. S. (1983). Assessment of secondary clarification design concepts. *Journal of Water Pollution Control Federation*, *55*(4), 349–359.

Ramalingam, K., Xanthos, S., Gong, M., Fillos, J., Beckmann, K., Deur, A., & McCorquodale, J. A. (2012). Critical modeling parameters identified for 3D CFD modeling of rectangular final settling tanks for New York City wastewater treatment plants. *Water Science and Technology*, *65*(6), 1087–1094. https://doi.org/10.2166/wst.2012.944

Stamou, A., & Gkesouli, A. (2015). Modeling settling tanks for water treatment using computational fluid dynamics. *Journal of Hydroinformatics*, *17*(5), 745–762.

Takács, I., Patry, G. G., & Nolasco, D. (1991). A dynamic model of the clarification-thickening process. *Water Research*, *25*(10), 1263–1271.

Tecplot 360. Bellevue, Washington, USA. Retrieved from https://www.tecplot.com/products/tecplot-360/

Trelis 16.5. American Fork, Utah, USA. Retrieved from https://www.csimsoft.com

Vitasovic, Z. C., Zhou, S., McCorquodale, J. A., & Lingren, K. (1997). Secondary clarifier analysis using data from the Clarifier Research Technical Committee protocol. *Water Environment Research*, *69*(5), 999–1007.

Wei, W., Liu, Y., & Lv, B. (2016). Numerical simulation of optimal submergence depth of impellers in an oxidation ditch. *Desalination and Water Treatment*, *57*(18), 8228–8235.

Weiss, M., Plósz, B. G., Essemiani, K., & Meinhold, J. (2007). Suction-lift sludge removal and non-Newtonian flow behaviour in circular secondary clarifiers: Numerical modelling and measurements. *Chemical Engineering Journal*, *132*(1–3), 241–255.

Wicklein, E., & Samstag, R. W. (2009). *Comparing commercial and transport CFD models for secondary sedimentation*. In Proceedings of WEFTEC 09–82th Annual WEF Technical Exhibition and Conference (pp. 6066–6081). Orlando, FL.

Zhou, S., & McCorquodale, J. A. (1992a). Influence of skirt radius on performance of circular clarifier with density stratification. *International Journal for Numerical Methods in Fluids*, *14*(8), 919–934. https://doi.org/10.1002/fld.1650140804

Zhou, S., & McCorquodale, J. A. (1992b). Mathematical modelling of a circular clarifier. *Canadian Journal of Civil Engineering*, *19*(3), 365–374.